



An Imperfectly Passive Nature: Bright Submillimeter Emission from Dust-obscured Star Formation in the $z = 3.717$ “Passive” System, ZF 20115

J. M. Simpson^{1,24}, Ian Smail², Wei-Hao Wang^{1,24}, D. Riechers³, J. S. Dunlop⁴, Y. Ao⁵, N. Bourne⁴, A. Bunker⁶, S. C. Chapman⁷, Chian-Chou Chen⁸, H. Dannerbauer^{9,10}, J. E. Geach¹¹, T. Goto¹², C. M. Harrison⁸, H. S. Hwang¹³, R. J. Ivison^{8,4}, Tadayuki Kodama⁵, C.-H. Lee¹⁴, H.-M. Lee¹⁵, M. Lee^{5,16}, C.-F. Lim^{1,24}, M. J. Michałowski^{4,17}, D. J. Rosario², H. Shim¹⁸, X. W. Shu¹⁹, A. M. Swinbank², W.-L. Tee^{1,20,24}, Y. Toba^{1,24}, E. Valiante²¹, Junxian Wang²², and X. Z. Zheng²³

¹ Academia Sinica Institute of Astronomy and Astrophysics, No. 1, Sec. 4, Roosevelt Road, Taipei 10617, Taiwan; jsimpson@asiaa.sinica.edu.tw

² Centre for Extragalactic Astronomy, Department of Physics, Durham University, South Road, Durham DH1 3LE, UK

³ Department of Astronomy, Cornell University, 220 Space Sciences Building, Ithaca, NY 14853, USA

⁴ Institute for Astronomy, University of Edinburgh, Royal Observatory, Blackford Hill, Edinburgh EH9 3HJ, UK

⁵ National Astronomical Observatory of Japan (NAOJ), 2-21-1 Osawa, Mitaka, Tokyo 181-8588, Japan

⁶ Department of Physics, University of Oxford, Denys Wilkinson Building, Keble Road, Oxford OX1 3RH, UK

⁷ Department of Physics and Atmospheric Science, Dalhousie University, Halifax, NS B3H 3J5, Canada

⁸ European Southern Observatory, Karl Schwarzschild Strasse 2, Garching, Germany

⁹ Instituto de Astrofísica de Canarias (IAC), E-38205 La Laguna, Tenerife, Spain

¹⁰ Universidad de La Laguna, Departamento de Astrofísica, E-38206 La Laguna, Tenerife, Spain

¹¹ Centre for Astrophysics Research, Science and Technology Research Institute, University of Hertfordshire, Hatfield AL10 9AB, UK

¹² Institute of Astronomy, National Tsing Hua University, No. 101, Sec. 2, Kuang-Fu Road, Hsinchu 30013, Taiwan

¹³ School of Physics, Korea Institute for Advanced Study, 85 Hoegiro, Dongdaemun-gu, Seoul 02455, Korea

¹⁴ Subaru Telescope, National Astronomical Observatory of Japan 650 N Aohoku Place, Hilo, HI 96720, USA

¹⁵ Department of Physics and Astronomy, Seoul National University, 1 Gwanak-ro, Gwanak-gu, Seoul 08826, Korea

¹⁶ Department of Astronomy, The University of Tokyo, 7-3-1 Hongo, Bunkyo-ku, Tokyo 133-0033, Japan

¹⁷ Astronomical Observatory Institute, Faculty of Physics, Adam Mickiewicz University, ul. Słoneczna 36, 60-286 Poznań, Poland

¹⁸ Department of Science Education, Kyungpook National University, 80 Daehakto, Bukgu, Daegu 41566, Korea

¹⁹ Department of Physics, Anhui Normal University, Wuhu, Anhui 241000, China

²⁰ Department of Physics, National Taiwan University, Taipei 10617, Taiwan

²¹ School of Physics and Astronomy, Cardiff University, Queen's Buildings, The Parade, Cardiff CF24 3AA, UK

²² Center for Astrophysics, University of Science & Technology of China, Hefei, Anhui 230026, China

²³ Purple Mountain Observatory, Chinese Academy of Sciences, 2 West Beijing Road, Nanjing 210008, China

Received 2017 April 10; revised 2017 June 7; accepted 2017 June 15; published 2017 July 19

Abstract

The identification of high-redshift, massive galaxies with old stellar populations may pose challenges to some models of galaxy formation. However, to securely classify a galaxy as quiescent, it is necessary to exclude significant ongoing star formation, something that can be challenging to achieve at high redshifts. In this Letter, we analyze deep ALMA/870 μm and SCUBA-2/450 μm imaging of the claimed “post-starburst” galaxy ZF 20115 at $z = 3.717$ that exhibits a strong Balmer break and absorption lines. The rest-frame far-infrared imaging identifies a luminous starburst $0''.4 \pm 0''.1$ (~ 3 kpc in projection) from the position of the ultraviolet/optical emission and is consistent with lying at the redshift of ZF 20115. The star-forming component, with an obscured star formation rate of $100^{+15}_{-70} M_{\odot} \text{ yr}^{-1}$, is undetected in the rest-frame ultraviolet but contributes significantly to the lower angular resolution photometry at rest-frame wavelengths $\gtrsim 3500 \text{ \AA}$. This contribution from the obscured starburst, especially in the *Spitzer*/IRAC wavebands, significantly complicates the determination of a reliable stellar mass for the ZF 20115 system, and we conclude that this source does not pose a challenge to current models of galaxy formation. The multi-wavelength observations of ZF 20115 unveil a complex system with an intricate and spatially varying star formation history. ZF 20115 demonstrates that understanding high-redshift obscured starbursts will only be possible with multi-wavelength studies that include high-resolution observations, available with the *James Webb Space Telescope*, at mid-infrared wavelengths.

Key words: galaxies: high-redshift – galaxies: starburst

1. Introduction

In the local universe, the most massive galaxies are giant spheroidal galaxies that formed the bulk of their stellar populations in a burst of star formation at $z \gtrsim 2$ (e.g., Nelan et al. 2005). Identifying the progenitors of these galaxies, in either a high-redshift passive or starburst phase, has become a major focus of galaxy formation surveys (e.g., Simpson et al. 2014; Straatman et al. 2014).

One route to isolating passive galaxies at high redshifts is to search for galaxies that have extremely red colors (e.g.,

$H-4.5 \mu\text{m} > 4$). These colors may arise due to the presence of a redshifted Balmer (3646 \AA) or 4000 \AA break in the spectral energy distribution (SED) of the source. However, the degeneracy between stellar age, redshift, and dust extinction means that proposed “passive” samples, selected on apparent colors, suffer high ($\gtrsim 80\%$) contamination from dusty interlopers at low and high redshift (Smail et al. 2002b; Toft et al. 2005; Boone et al. 2011; Caputi et al. 2012). Indeed, an early attempt to identify a $z > 3$ passive galaxy was presented by Mobasher et al. (2005), who claimed the detection of a bright post-starburst galaxy at $z \sim 6.5$. Dunlop et al. (2007) subsequently showed that allowing for extreme values of dust

²⁴ EACOA Fellow.

obscuration in the SED model yields a high likelihood that the source is a $z \sim 2$ dusty starburst.

Despite these challenges, a number of studies have continued to claim the detection of large numbers of passive galaxies at high redshift from wide-field near-infrared imaging (Marchesini et al. 2010; Nayyeri et al. 2014). The most massive of these are thought to have stellar masses of $\gtrsim 10^{11} M_{\odot}$ at $z \gtrsim 3$ that, if correct, may pose challenges for models of galaxy formation. However, a convincing spectroscopic confirmation of a truly massive, quiescent galaxy at $z \gtrsim 3$ has yet to be presented.

Recently, Glazebrook et al. (2017) presented deep near-infrared spectroscopy of ZF 20115, a purported “passive” galaxy at $z = 3.717$. ZF 20115 was selected from the ZFOURGE survey based on the presence of a strong Balmer break identified in near-infrared photometry (Straatman et al. 2014). Near-infrared spectroscopy then confirmed Balmer absorption lines with high equivalent width (EW) that were suggested to show that ZF 20115 is a “post-starburst” galaxy with a stellar age of 0.2–1 Gyr. The Balmer lines, combined with fits to the broadband photometry, led Glazebrook et al. (2017) to conclude in favor of an age in the range 0.5–1 Gyr, corresponding to a formation redshift $z_{\text{form}} \sim 5$ –8. Combined with the estimated stellar mass of 1.5 – $1.8 \times 10^{11} M_{\odot}$, this indicates a rapid conversion of baryons into stars at high redshift, as expected from studies of submillimeter galaxies (SMGs; e.g., Lilly et al. 1999; Smail et al. 2002a).

In this Letter, we analyze submillimeter observations of ZF 20115 with SCUBA-2 and ALMA, which identify an intense, obscured starburst within $0''.4 \pm 0''.1$ of the rest-frame ultraviolet component (ZF 20115-UV). Throughout, we adopt a Λ CDM cosmology with $H_0 = 70 \text{ km s}^{-1} \text{ Mpc}^{-1}$, $\Omega_{\Lambda} = 0.7$, and $\Omega_{\text{m}} = 0.3$ and a Chabrier initial mass function (Chabrier 2003).

2. Observations

The galaxy ZF 20115, located in the CANDELS region of the COSMOS field, was selected based on its rest-frame optical color in the ZFOURGE survey, and we use this photometric catalog in our analysis (Straatman et al. 2016).

ZF 20115 was observed in ALMA Cycle 2 at $870 \mu\text{m}$ for 1.4 minutes as part of program 2013.1.01292.S. The ALMA observations reach a depth of $\sigma_{870} = 0.2 \text{ mJy beam}^{-1}$, with a synthesized beam of $1''.1 \times 0''.6$, and reveal a significant (6.9σ) source (called ZF 20115-FIR hereafter) within $0''.4 \pm 0''.1$ of ZF 20115-UV (see also Glazebrook et al. 2017). We use CASA/IMFIT to model the emission and determine that ZF 20115-FIR is unresolved with a total flux density of $1.4 \pm 0.2 \text{ mJy beam}^{-1}$.

The central area of the CANDELS/COSMOS is being mapped at 450 and $850 \mu\text{m}$ by the SCUBA-2 Ultra Deep Imaging EAO Survey (STUDIES; PI: W.-H. Wang), a large program at the *James Clerk Maxwell Telescope* (JCMT). We make use of the first STUDIES release, which reaches a depth of $\sigma_{450} \sim 1 \text{ mJy}$ in the vicinity of the ZF 20115.²⁵ We detect ZF 20115-FIR at a 3σ significance level in the $450 \mu\text{m}$ imaging, identifying a $S_{450} = 3.1 \pm 1.0 \text{ mJy}$ source within the expected 1σ positional uncertainty ($2''.1$; Ivison et al. 2007). ZF 20115-FIR is detected in the STUDIES SCUBA-2 $850 \mu\text{m}$ imaging with a flux density of $S_{850} = 1.49 \pm 0.15 \text{ mJy}$, consistent with the ALMA detection.

The CANDELS/COSMOS region was imaged with *Herschel*/PACS and SPIRE as part of the *Herschel*-CANDELS

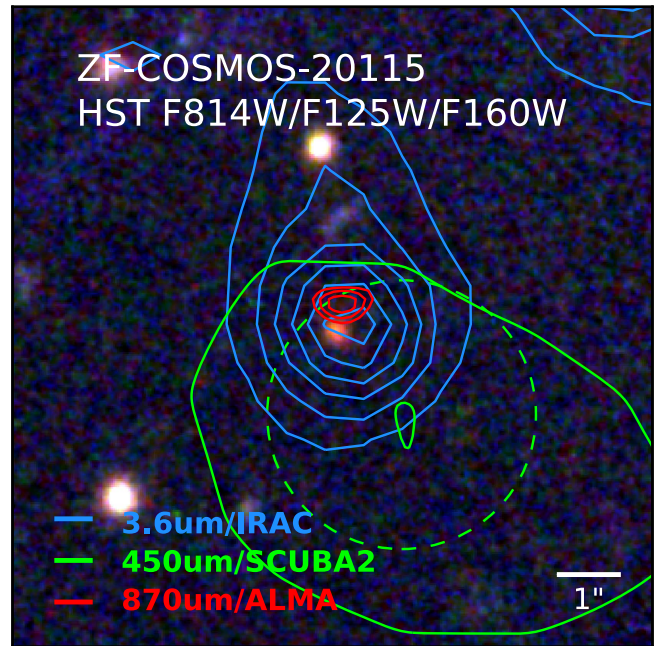


Figure 1. *HST* true color image ($I_{814}J_{125}H_{160}$) of ZF 20115 overlaid with contours representing ALMA/ $870 \mu\text{m}$ ($\pm 4, 5 \dots \times \sigma$), SCUBA-2/ $450 \mu\text{m}$ ($\pm 2, 3 \times \sigma$), and IRAC/ $3.6 \mu\text{m}$ ($\pm 5, 10, 15 \dots \times \sigma$) emission. The 1σ positional uncertainty on the $450 \mu\text{m}$ detection is represented by a dashed circle. The ALMA emission is offset by $0''.4 \pm 0''.1$ ($\sim 3 \text{ kpc}$ in projection) to the rest-frame ultraviolet-to-optical emission, consistent with *HST* observations of high-redshift dusty starbursts (Chen et al. 2015). The $3.6 \mu\text{m}$ /IRAC emission appears extended in the direction of the far-infrared emission, highlighting that the near-infrared photometry of ZF 20115 likely comprises a blend of the unobscured and obscured components.

survey and *Herschel* Multi-tiered Extragalactic Survey (HerMES; Oliver et al. 2012). Straatman et al. (2014) present the PACS photometry for ZF 20115, with stated 1σ uncertainties of 0.4 mJy at 100 and $160 \mu\text{m}$. At $160 \mu\text{m}$ the claimed depth is below the measured confusion limit of PACS, but it is not possible to verify this as the reduced *Herschel*-CANDELS imaging is not publicly available and the data reduction is not detailed in the literature. The deblended SPIRE imaging reaches 1σ depths of $3.1, 3.5$, and 4.1 mJy at $250, 350$, and $500 \mu\text{m}$ (Swinbank et al. 2014). ZF 20115 is not detected in the 100 – $500 \mu\text{m}$ imaging. Finally, ZF 20115 is not detected in the available 1.4 and 3 GHz imaging (Schinnerer et al. 2010; Smolcic et al. 2017), consistent with lying at a redshift of $z \gtrsim 2.5$.

We align the astrometry of the wide-field imaging presented here by correcting for the mean offset between the *Spitzer* IRAC/ $3.6 \mu\text{m}$ image and the relevant image. We cannot apply this technique to the single ALMA pointing, but we note that the overall ALMA astrometry has been found to be in agreement with the solution for the CANDELS/COSMOS imaging (Schreiber et al. 2017).

3. Analysis

In Figure 1, we show the archival ALMA $870 \mu\text{m}$ data for ZF 20115, contoured on the *HST*/CANDELS imaging. We first consider that the observed $870 \mu\text{m}$ emission (ZF 20115-FIR) is located $0''.4 \pm 0''.1$ ($\sim 3 \text{ kpc}$ in projection) from the detected rest-frame UV emission. At the redshift of ZF 20115-UV

²⁵ Including archival data from Geach et al. (2017).

($z = 3.717$) the near-infrared wavebands ($\lesssim 2.0 \mu\text{m}$) trace rest-frame ultraviolet emission, and thus it is unsurprising to find positional offsets between obscured and unobscured components. Indeed, the measured offset between ZF 20115-UV and ZF 20115-FIR is consistent with Chen et al. (2015), who determine an *intrinsic* offset between the *HST*- and ALMA-traced emission in SMGs of $0''.55$ (1σ), evidence for structured dust obscuration in these sources (Chapman et al. 2004; Hodge et al. 2015).

To test whether ZF 20115-UV and ZF 20115-FIR are physically associated, we calculate the probability that they arise due to the chance alignment of two sources on the sky. First, we create mock catalogs with source surface densities that satisfy the ZFOURGE color-criterion for a massive, quiescent galaxy (Straatman et al. 2014) and submillimeter sources at $S_{870} > 1 \text{ mJy}$ (Dunlop et al. 2017). We do not account for any bias due to gravitational lensing but comment that this is unlikely given that ZF 20115 is located at $z = 3.717$. From these mock catalogs we determine a probability of $\sim 1.5 \times 10^{-4}$ that ZF 20115-UV and ZF 20115-FIR are a chance alignment, in agreement with the corrected Poissonian probability (Downes et al. 1986). Given this low probability and the similarity with the properties of high-redshift dusty starbursts, we conclude that ZF 20115 is most likely a composite dusty starburst.

3.1. Properties of the Starburst

To determine the far-infrared properties of ZF 20115-FIR, we fit the far-infrared photometry with a single-temperature, optically thin, modified blackbody (mBB) function. The $100 \mu\text{m}$ photometry (rest-frame $\sim 20 \mu\text{m}$) is dominated by polycyclic aromatic hydrocarbon features and is not included in our SED fitting. The dust emissivity is fixed at $\beta = 1.8$, and the best-fit parameters and associated uncertainties are determined using a Monte Carlo Markov Chain (MCMC) approach (Simpson et al. 2017), accounting for the effect of the cosmic microwave background following da Cunha et al. (2013).

Our SED fitting shows that ZF 20115-FIR has a best-fit dust temperature of $T_d = 30.4^{+1.4}_{-12.0} \text{ K}$ and a far-infrared luminosity ($8\text{--}1000 \mu\text{m}$) of $L_{\text{FIR}} = 7.7^{+1.0}_{-5.2} \times 10^{11} L_{\odot}$. A single-temperature mBB is known to underestimate the total far-infrared luminosity by $\sim 20\%$ (Swinbank et al. 2014), and correcting for this, we determine that ZF 20115 has a total far-infrared luminosity of $L_{\text{FIR}} = 9.2^{+1.2}_{-6.2} \times 10^{11} L_{\odot}$ and an obscured star formation rate (SFR) of $100^{+15}_{-70} M_{\odot} \text{ yr}^{-1}$ (Kennicutt 1998).

4. Discussion

Interest in ZF 20115 (e.g., Rong et al. 2017) has arisen due to the claim that its stellar population is massive and quiescent at $z = 3.717$ (Glazebrook et al. 2017). We now reassess the properties of ZF 20115, accounting for the presence of an obscured starburst, blended or co-located, with the rest-frame UV emission.

4.1. Origin of Balmer Absorption Lines

Near-infrared spectroscopy of ZF 20115 identified Balmer absorption lines with a combined EW of $38 \pm 6 \text{ \AA}$ (summing $\text{H}\beta$, $\text{H}\gamma$, and $\text{H}\delta$; Glazebrook et al. 2017). This requires that the detectable stellar continuum around $4000\text{--}5000 \text{ \AA}$ is dominated by A-stars with lifetimes of $\sim 0.1\text{--}1 \text{ Gyr}$ and is often taken as

an indicator of a “post-starburst” population. However, Balmer absorption features are not unique to post-starburst galaxies; they appear frequently in dusty starburst galaxies (Poggianti & Wu 2000).

Poggianti & Wu (2000) present detections of the $\text{H}\delta$ absorption line for a sample of *IRAS*-selected galaxies ($L_{\text{FIR}} > 5 \times 10^{11} L_{\odot}$) at $z \lesssim 0.05$. This far-infrared-bright sample is dominated by star-forming galaxies, and over 60% show evidence of ongoing interactions or mergers. In Figure 2, we show the SED of Mrk 331 (Brown et al. 2014) from the sample of Poggianti & Wu (2000), scaled in luminosity to match ZF 20115. Mrk 331 is a late-stage merger and exhibits $\text{H}\delta$ absorption with $\text{EW} = 4.1 \text{ \AA}$ and a strong break at $\lesssim 4000 \text{ \AA}$. We note that few local examples reach the high EW Balmer absorption observed from ZF 20115 but comment that this may be a reflection of the low survey volumes and decreased activity at $z \sim 0$ (see, e.g., Smail et al. 1999). The SED of Mrk 331 is in qualitative agreement with that of ZF 20115, illustrating the challenge of deriving accurate star formation histories for high-redshift “red” galaxies from optical-to-near-infrared photometry alone (see also Charmandaris et al. 2004).

The high EW Balmer absorption features that appear common in starburst galaxies can be explained by age-dependant dust obscuration (Poggianti & Wu 2000). This can be considered in terms of a single isolated galaxy, or triggered star formation in an ongoing merger. Given the presence of two components with a projected offset of 3 kpc, we suggest that the ZF 20115 system is an ongoing merger between two gas-rich progenitors. In this scenario, the centroid of the *observable* stellar emission likely traces one component of the merger that underwent a burst of star formation, triggered by an earlier interaction.

Hopkins et al. (2013) present numerical simulations of the merger of gas-rich disks at high redshift, which demonstrate that star formation is triggered in the individual disks $\sim 0.5 \text{ Gyr}$ before coalescence and the triggering of a nuclear starburst. The Balmer absorption in the spectrum of ZF 20115 is likely the consequence of a similar merger event, with the strength of the lines indicating a minimum age for this initial star formation episode of $\sim 100 \text{ Myr}$ (González Delgado et al. 1999; Glazebrook et al. 2017).

4.2. Stellar Mass of ZF 20115

The detection by ALMA of a strongly star-forming, obscured component within $0''.4 \pm 0''.1$ of the claimed quiescent component ZF 20115-UV significantly complicates the analysis of this system. To some extent, the issue about whether the two components are part of a single “galaxy” or are distinct components within a larger halo is one of semantics. What is unarguable is that the presence of this luminous, star-forming component will result in significant contamination of the flux measurements in longer-wavelength bands, which are critical for estimating the stellar mass of the system. At the redshift of ZF 20115, the stellar emission from the obscured starburst peaks in the $2''$ resolution *Spitzer*/IRAC imaging (rest-frame $0.8\text{--}1.7 \mu\text{m}$), where the two components are strongly blended (Figure 1). At these wavelengths, the mass-to-light ratio of a stellar population varies by an order of magnitude for ages of $50\text{--}1000 \text{ Myr}$ (Hainline et al. 2011), and so it is crucial that we take the contribution from ZF 20115-UV into account.

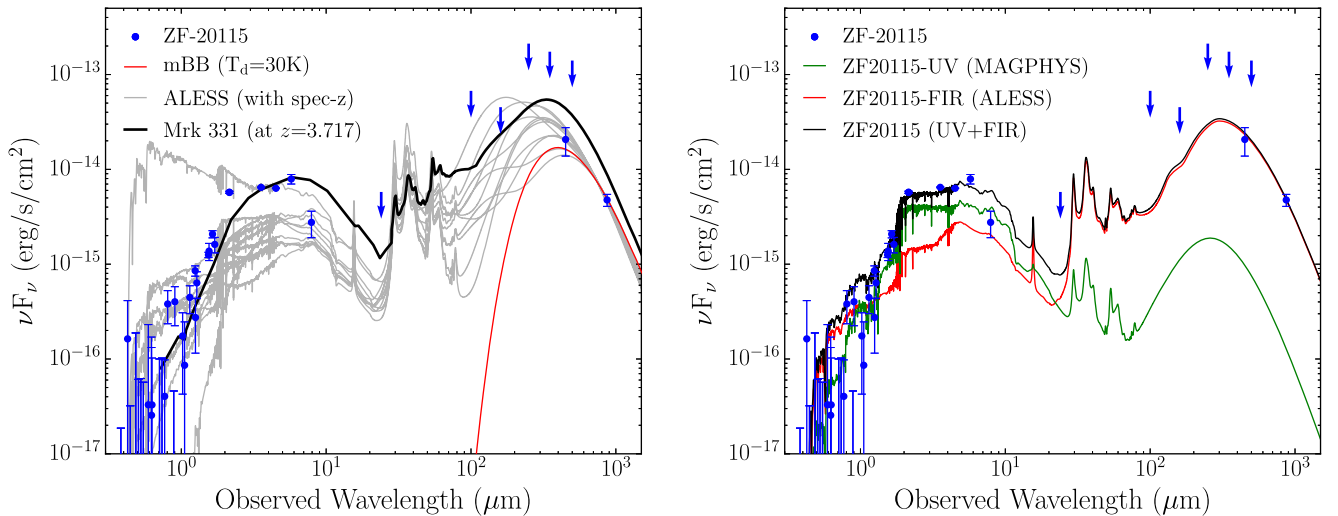


Figure 2. Observed photometry of ZF 20115 as a function of observed wavelength (arrows represent 3σ upper limits). Left: the best-fit mBB function to the far-infrared photometry is shown, corresponding to an obscured SFR of $100^{+15}_{-70} M_{\odot} \text{ yr}^{-1}$, and we overlay SEDs derived for a subset of the spectroscopically confirmed ALESS SMGs (Danielson et al. 2017). The model SED of Mrk 331 is shown, redshifted to $z = 3.717$ and scaled to broadly match ZF 20115. This local far-infrared-bright starburst is an ongoing merger and has detected $H\beta$ and $H\delta$ in absorption and a strong Balmer break, illustrating that Balmer features do not uniquely identify “post-starburst” galaxies. Right: decomposition of the ZF 20115 system into unobscured and obscured components. The average SED created from the best-fit ALESS SMG templates is shown, indicating the significant contribution that the obscured starburst makes to the overall optical-to-near-infrared photometry (20%–75%). We deblend the photometry of the ZF 20115 system by subtracting the average SMG and modeling the residual photometry with MAGPHYS. From the deblended photometry, we estimate that ZF 20115-UV has a stellar mass of $\sim 0.8 \times 10^{11} M_{\odot}$, less than half that estimated from modeling the system as a single, unobscured component.

We use two methods to estimate the likely contribution from ZF 20115-FIR to the integrated photometry. First, we deblend the $3.6/4.5 \mu\text{m}$ emission using three 2D Gaussian components representing ZF 20115-UV, ZF 20115-FIR, and the northern optically bright galaxy (Figure 1). We determine that ZF 20115-FIR contributes $\sim 40\%$ – 50% of the integrated flux density at 3.6 and $4.5 \mu\text{m}$, consistent with the two components being indistinguishable in the IRAC imaging. Second, we estimate the contribution by considering the spectroscopically identified, ALMA-located-SMGs from Danielson et al. (2017). We fit the templates for these SMGs to the far-infrared photometry of ZF 20115-FIR, and in Figure 2 show those SEDs that are near-infrared-bright and have far-infrared properties matching ZF 20115-FIR. We create an average SED from these best-fit templates and estimate that the obscured starburst contributes 25%–70% (median $34 \pm 5\%$) of the measured photometry of ZF 20115 at observed 1.5 – $8.0 \mu\text{m}$,²⁶ broadly consistent with our estimates from deblending the IRAC imaging.

To estimate the mass of the stellar component associated with ZF 20115-UV, we subtract the average starburst SED from the global photometry. Using MAGPHYS (da Cunha et al. 2015) to model the residual photometry, we estimate that this component has a stellar mass of $\sim 0.8 \times 10^{11} M_{\odot}$, less than half of that estimated by Glazebrook et al. (2017). We cannot determine an accurate star formation history for this component but note that a rapid formation at high redshift ($z \gtrsim 5$) is no longer required and that the implied SFR and duration are consistent with the population of obscured starbursts that are known at $z \gtrsim 4$ (e.g., Riechers et al. 2013; Simpson et al. 2017; Strandet et al. 2016). Using the stellar mass estimates presented by Danielson et al. (2017), we estimate that ZF 20115-FIR has

a mass of $\sim 0.4 \times 10^{11} M_{\odot}$. At the current SFR and assuming a constant star formation history, this stellar component could form in ~ 350 Myr, equivalent to a formation redshift of $z = 3.7$ – 4.6 .

The apparent quiescent nature of ZF 20115 led Glazebrook et al. (2017) to suggest that this source, and the parent sample of proposed quiescent galaxies, may be in conflict with current models of galaxy formation (e.g., Steinhardt et al. 2016). The contamination of the stellar mass estimates for ZF 20115-UV has implications for the conclusions presented by Glazebrook et al. (2017), and we revisit those here.

First, we adopt the halo mass of $\sim 3 \times 10^{12} M_{\odot}$ for ZF 20115 estimated by Glazebrook et al. (2017). Assuming a cosmic baryon fraction of 16% (Planck Collaboration et al. 2016), we estimate that the stellar mass for ZF 20115-UV corresponds to a baryon conversion efficiency of $\sim 15\%$ – 40% , at a formation redshift of $z_{\text{form}} = 4$ – 5 . Genel et al. (2014) demonstrate that comparable halos in the Illustris simulation have a conversion efficiency of $\sim 10\%$ at $z \sim 4$, consistent with observational studies of UV-selected galaxies (Finkelstein et al. 2015). The conversion of baryons into stars appears to be progressing more efficiently in ZF 20115-UV, although it remains well below the theoretical limit. Indeed, simulations of galaxy formation do predict the presence of $z \sim 4$ star-forming systems with stellar masses of $\sim 10^{11} M_{\odot}$ (Wellons et al. 2015; Rodriguez-Gomez et al. 2016), at a space density in agreement with observational studies (e.g., Mortlock et al. 2017). Thus, while ZF 20115 remains an interesting system, it does not appear to be in conflict with our understanding of galaxy formation.

5. Conclusions

In this Letter, we have analyzed ALMA and SCUBA-2 observations of ZF 20115, a proposed massive, quiescent galaxy at $z = 3.717$. The rest-frame far-infrared imaging

²⁶ Corresponds to $L_{\text{FIR}} = 1.5 \pm 0.2 \times 10^{11} L_{\odot}$ (SFR = $160 \pm 20 M_{\odot} \text{ yr}^{-1}$), consistent with the best-fit mBB.

locates an obscured starburst only $0''.4 \pm 0''.1$ from the unobscured ZF 20115-UV. As we show, the far-infrared luminous starburst appears associated with ZF 20115-UV bringing into doubt the claim that this is a quiescent system. Indeed, the Balmer absorption features exhibited by ZF 20115 are not a unique tracer of a “post-starburst” galaxy and appear frequently in local *IRAS*-selected starbursts (Poggianti & Wu 2000).

ZF 20115-UV and ZF 20115-FIR are separated by ~ 3 kpc on the sky, a strong indication that they may reside within the same halo and are consistent with *HST* studies of ALMA-identified SMGs at these redshifts. While the question of whether these components represent a single “galaxy” is one of semantics, it is unavoidable that the presence of a starburst within $0''.4 \pm 0''.1$ of ZF 20115-UV means that allowance must be made for blending in the low spatial resolution SED of this system, particularly at long wavelengths.

Including a dusty starburst component in the SED fitting of ZF 20115 indicates that $\sim 30\%$ – 50% of the total rest-frame $1\text{--}2\ \mu\text{m}$ emission arises from the ongoing starburst. Correcting for this contribution and refitting the SED, we determine that ZF 20115-UV has a stellar mass of $\sim 0.8 \times 10^{11} M_{\odot}$, although we stress that the uncertainties on this measurement are large. The corrected stellar mass is $\sim 50\%$ lower than previously published values and, as we show, this removes the tension between ZF 20115 and models of galaxy formation.

The multi-wavelength imaging and spectroscopy of the ZF 20115 system provides key insights into the properties of obscured starbursts at high redshifts. ZF 20115 comprises a blend of obscured and unobscured components that host intense, but spatially variable, star formation. The strength of the Balmer absorption features suggest that the system has a complex star formation history and was undergoing a star formation event at least 100 Myr prior to the current episode. This can be explained by adopting a merger model for the system, but is challenging to understand if secular processes dominate the formation mechanism of high-redshift starbursts. What is clear from our analysis is that to untangle this complex system, and thus truly understand high-redshift starbursts, we require the high-resolution imaging at mid-infrared wavelengths that will only be available with the *James Webb Space Telescope*.

The authors thank Nick Scoville for sharing his catalog of ALMA observations and Alice Shapley for helpful comments. J.M.S. acknowledges an EACOA fellowship. I.R.S. acknowledges support from DUSTYGAL 321334, an RS/Wolfson Merit Award and STFC (ST/P000541/1). D.R. acknowledges support under grant number AST-1614213.

This Letter makes use of data taken with SCUBA-2/JCMT and ALMA (ADS/JAO.ALMA#2013.1.01292.S). The JCMT is operated by the EAO on behalf of NAOJ, ASIAA, KASI,

NOAC, and CAS, with additional support from STFC/U.K. and participating universities in the United Kingdom and Canada.

References

- Boone, F., Schaerer, D., Pelló, R., et al. 2011, *A&A*, **534**, A124
 Brown, M. J. I., Moustakas, J., Smith, J.-D. T., et al. 2014, *ApJS*, **212**, 18
 Caputi, K. I., Dunlop, J. S., McLure, R. J., et al. 2012, *ApJL*, **750**, L20
 Chabrier, G. 2003, *PASP*, **115**, 763
 Chapman, S. C., Smail, I., Windhorst, R., Muxlow, T., & Ivison, R. J. 2004, *ApJ*, **611**, 732
 Charmandaris, V., Le Floch, E., & Mirabel, I. F. 2004, *ApJL*, **600**, L15
 Chen, C.-C., Smail, I., Swinbank, A. M., et al. 2015, *ApJ*, **799**, 194
 da Cunha, E., Groves, B., Walter, F., et al. 2013, *ApJ*, **766**, 13
 da Cunha, E., Walter, F., Smail, I. R., et al. 2015, *ApJ*, **806**, 110
 Danielson, A. L. R., Swinbank, A. M., Smail, I., et al. 2017, *ApJ*, **840**, 78
 Downes, A. J. B., Peacock, J. A., Savage, A., & Carrie, D. R. 1986, *MNRAS*, **218**, 31
 Dunlop, J. S., Cirasuolo, M., & McLure, R. J. 2007, *MNRAS*, **376**, 1054
 Dunlop, J. S., McLure, R. J., Biggs, A. D., et al. 2017, *MNRAS*, **466**, 861
 Finkelstein, S. L., Song, M., Behroozi, P., et al. 2015, *ApJ*, **814**, 95
 Geach, J. E., Dunlop, J. S., Halpern, M., et al. 2017, *MNRAS*, **465**, 1789
 Genel, S., Vogelsberger, M., Springel, V., et al. 2014, *MNRAS*, **445**, 175
 Glazebrook, K., Schreiber, C., Labbé, I., et al. 2017, *Natur*, **544**, 71
 González Delgado, R. M., Leitherer, C., & Heckman, T. M. 1999, *ApJS*, **125**, 489
 Hainline, L. J., Blain, A. W., Smail, I., et al. 2011, *ApJ*, **740**, 96
 Hodge, J. A., Riechers, D., Decarli, R., et al. 2015, *ApJL*, **798**, L18
 Hopkins, P. F., Cox, T. J., Hernquist, L., et al. 2013, *MNRAS*, **430**, 1901
 Ivison, R. J., Greve, T. R., Dunlop, J. S., et al. 2007, *MNRAS*, **380**, 199
 Kennicutt, R. C. 1998, *ARA&A*, **36**, 189
 Lilly, S. J., Eales, S. A., Gear, W. K. P., et al. 1999, *ApJ*, **518**, 641
 Marchesini, D., Whitaker, K. E., Brammer, G., et al. 2010, *ApJ*, **725**, 1277
 Mobasher, B., Dickinson, M., Ferguson, H. C., et al. 2005, *ApJ*, **635**, 832
 Mortlock, A., McLure, R. J., Bowler, R. A. A., et al. 2017, *MNRAS*, **465**, 672
 Nayyeri, H., Mobasher, B., Hemmati, S., et al. 2014, *ApJ*, **794**, 68
 Nelán, J. E., Smith, R. J., Hudson, M. J., et al. 2005, *ApJ*, **632**, 137
 Oliver, S. J., Bock, J., Altieri, B., et al. 2012, *MNRAS*, **424**, 1614
 Planck Collaboration, Ade, P. A. R., Aghanim, N., et al. 2016, *A&A*, **594**, A13
 Poggianti, B. M., & Wu, H. 2000, *ApJ*, **529**, 157
 Riechers, D. A., Bradford, C. M., Clements, D. L., et al. 2013, *Natur*, **496**, 329
 Rodríguez-Gómez, V., Pillepich, A., Sales, L. V., et al. 2016, *MNRAS*, **458**, 2371
 Rong, Y., Jing, Y., Gao, L., et al. 2017, arXiv:1704.00012
 Schinnerer, E., Sargent, M. T., Bondi, M., et al. 2010, *ApJS*, **188**, 384
 Schreiber, C., Pannella, M., Leiton, R., et al. 2017, *A&A*, **599**, A134
 Simpson, J. M., Smail, I., Swinbank, A. M., et al. 2017, *ApJ*, **839**, 58
 Simpson, J. M., Swinbank, A. M., Smail, I., et al. 2014, *ApJ*, **788**, 125
 Smail, I., Ivison, R. J., Blain, A. W., & Kneib, J.-P. 2002a, *MNRAS*, **331**, 495
 Smail, I., Morrison, G., Gray, M. E., et al. 1999, *ApJ*, **525**, 609
 Smail, I., Owen, F. N., Morrison, G. E., et al. 2002b, *ApJ*, **581**, 844
 Smolcic, V., Novak, M., Bondi, M., et al. 2017, arXiv:1703.09713
 Steinhardt, C. L., Capak, P., Masters, D., & Speagle, J. S. 2016, *ApJ*, **824**, 21
 Straatman, C. M. S., Labbé, I., Spitler, L. R., et al. 2014, *ApJL*, **783**, L14
 Straatman, C. M. S., Spitler, L. R., Quadri, R. F., et al. 2016, *ApJ*, **830**, 51
 Strandet, M. L., Weiss, A., Vieira, J. D., et al. 2016, *ApJ*, **822**, 80
 Swinbank, A. M., Simpson, J. M., Smail, I., et al. 2014, *MNRAS*, **438**, 1267
 Toft, S., van Dokkum, P., Franx, M., et al. 2005, *ApJL*, **624**, L9
 Wellons, S., Torrey, P., Ma, C.-P., et al. 2015, *MNRAS*, **449**, 361